

Jonathan S. Huff<sup>†</sup>, Paul H. Davis<sup>†</sup>, Allison Christy<sup>†</sup>, Donald L. Kellis<sup>†</sup>, Nirmala Kandadai<sup>§</sup>, Bernard Yurke<sup>\*†§</sup>, William B. Knowlton<sup>\*†§</sup>, and Ryan D. Pensack<sup>\*†</sup>

<sup>†</sup>Micron School of Materials Science & Engineering, <sup>‡</sup>Department of Chemistry & Biochemistry, and <sup>§</sup>Department of Electrical & Computer Engineering, Boise State University, Boise, Idaho 83725, United States  
(\*e-mail: [bernardyurke@boisestate.edu](mailto:bernardyurke@boisestate.edu) (B.Y.), [bknowlton@boisestate.edu](mailto:bknowlton@boisestate.edu) (W.B.K.), & [ryanpensack@boisestate.edu](mailto:ryanpensack@boisestate.edu) (R.D.P.))

## 1. INTRODUCTION

### Motivation & Background

- Dye aggregates, which are most readily identified by spectral shifts in their absorption spectrum relative to the isolated dye,[1-3] can exhibit interesting photophysics including small Stokes shifts, superradiance, and long-range coherent energy transport.[4-6]
- Templated assembly of dye aggregates via covalent attachment of dye molecules to a DNA scaffold (DNA templating) is a promising strategy for controlled dye aggregation.[7-11]
- We studied the excited state dynamics of three DNA templated Cy5 structures: a monomer, a dimer, and a tetramer (See Figure 1).[12]

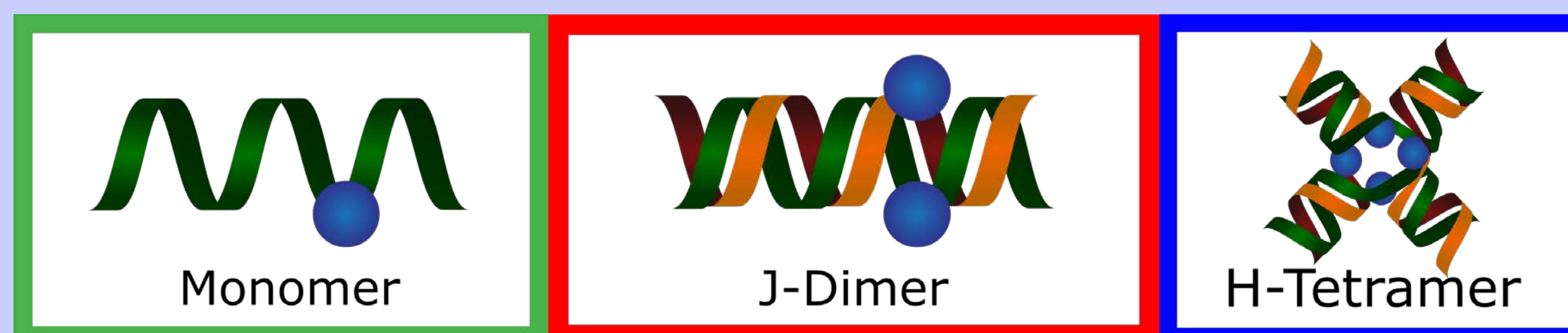


**Figure 1.** The three DNA templated dye structures we studied in this work. (Left) The monomer structure consists of a 26 base oligonucleotide with a single Cy5 attachment. (Middle) the J-dimer results from the hybridization of the monomer structure with its Cy5 labeled complement. (Right) The H-tetramer forms at high salt concentration through the association of two J-dimer structures.[8]

- In our primary poster, we report the extracted fluorescence emission spectrum of the J-dimer species, as well as the contribution of nonradiative decay to the overall relaxation dynamics of the aggregate structures.
- This poster presents additional details of the emission spectrum extraction, which accounts for the presence of two subpopulations in the J-dimer solution. Additional detail regarding the estimation of nonradiative decay in the aggregates is also presented.
- In both cases, the expected photophysical properties of small dye aggregates is leveraged to place bounded estimates on photophysical quantities which cannot be directly measured.

## 2. IDENTIFICATION OF MONOMER SUBPOPULATION

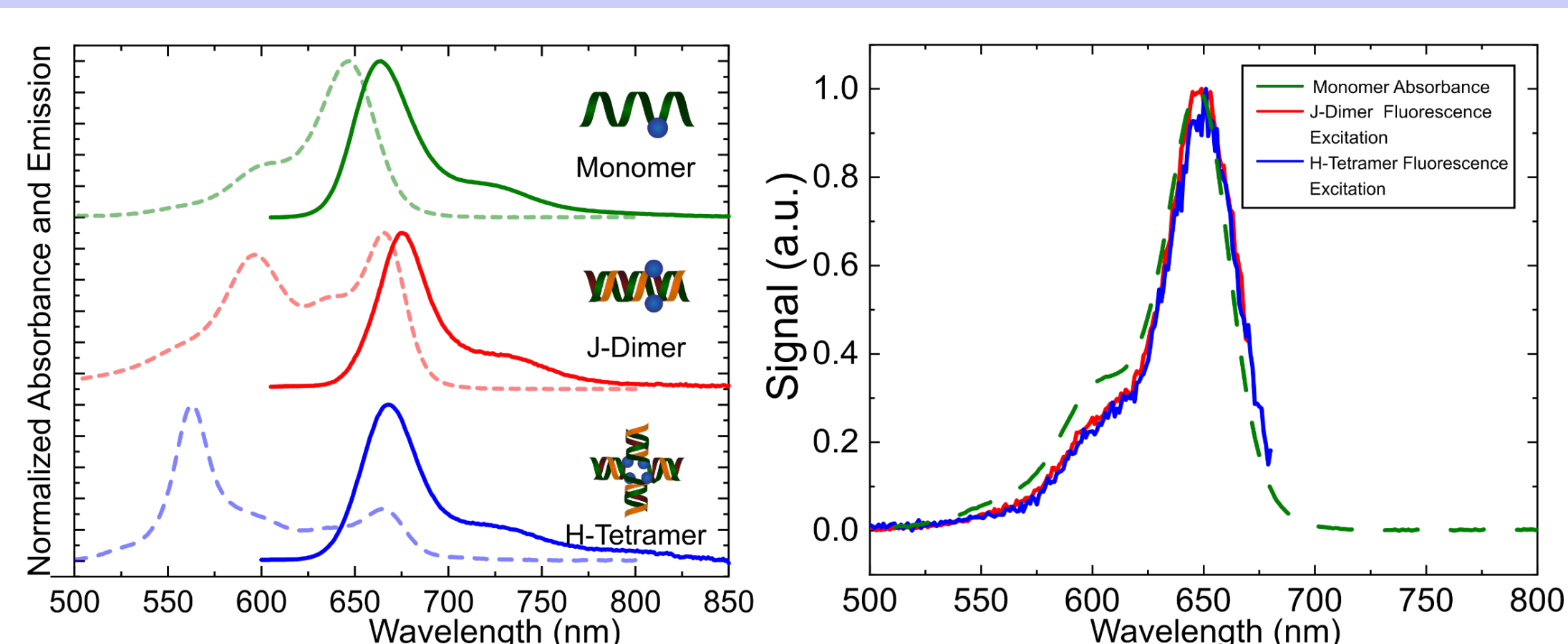


**Figure 2.** (Left) Fluorescence emission spectra (solid lines) and visible absorption spectra (dashed lines) of the Cy5 monomer (green), J-dimer (red), and H-tetramer (blue) solutions. (Right) Fluorescence excitation spectra of the aggregate solutions (solid lines) compared to the absorption spectrum of the Cy5 monomer (dashed line). The emission for both aggregate solutions was collected at 700 nm while the excitation wavelength was scanned.

- The emission spectra of the Cy5 aggregate solutions (Figure 2, left) resemble the Cy5 monomer emission spectrum and lack mirror symmetry with their respective absorption spectra, possibly suggesting a monomer subpopulation.
- A Cy5 monomer subpopulation was confirmed through fluorescence excitation measurements of the aggregate solutions (Figure 2, right). The J-dimer and H-tetramer fluorescence excitation spectra strongly resemble the monomer absorption spectrum, indicating that the Cy5 monomer is the primary emissive species in the aggregate solutions despite their low concentration.

## 3. IDENTIFICATION OF H-AGGREGATE SUBPOPULATION IN J-DIMER SOLUTION

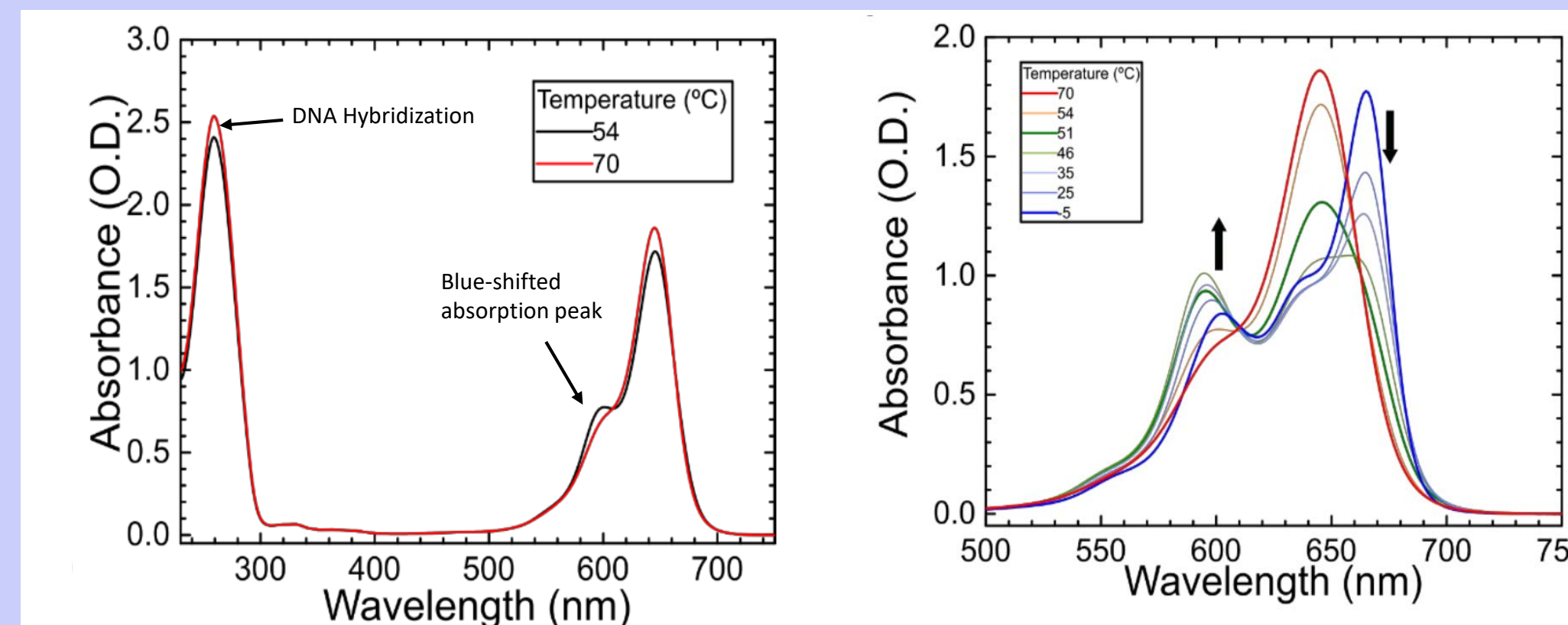


**Figure 3.** (Left) Absorption spectra collected on a J-dimer solution (red) above the denaturation temperature, and just below the denaturation temperature (black). (Right) Absorption spectra of the J-dimer collected at temperatures between -5 °C (dark blue) and 70 °C (red). Reproduced from [12]

- A solution of J-dimer was heated to 70 °C to denature the duplex.
- Upon cooling, an absorption feature at 597 nm appears just below denaturation temperature (54 °C), while the strongest absorption feature at 666 nm of the room temperature J-dimer solution is absent.
- Below the DNA denaturation temperature, the 597 nm and 666 nm absorption peaks change counter to one another under varied temperature.
- The spectra collected below the denaturation temperature exhibit isosbestic points at 604.5 and 610 nm.
- The presence of a new band at 597 nm and the presence of isosbestic points indicate the presence of an additional small H-aggregate subpopulation in the solution.

## 4. J-DIMER EMISSION SPECTRUM EXTRACTION

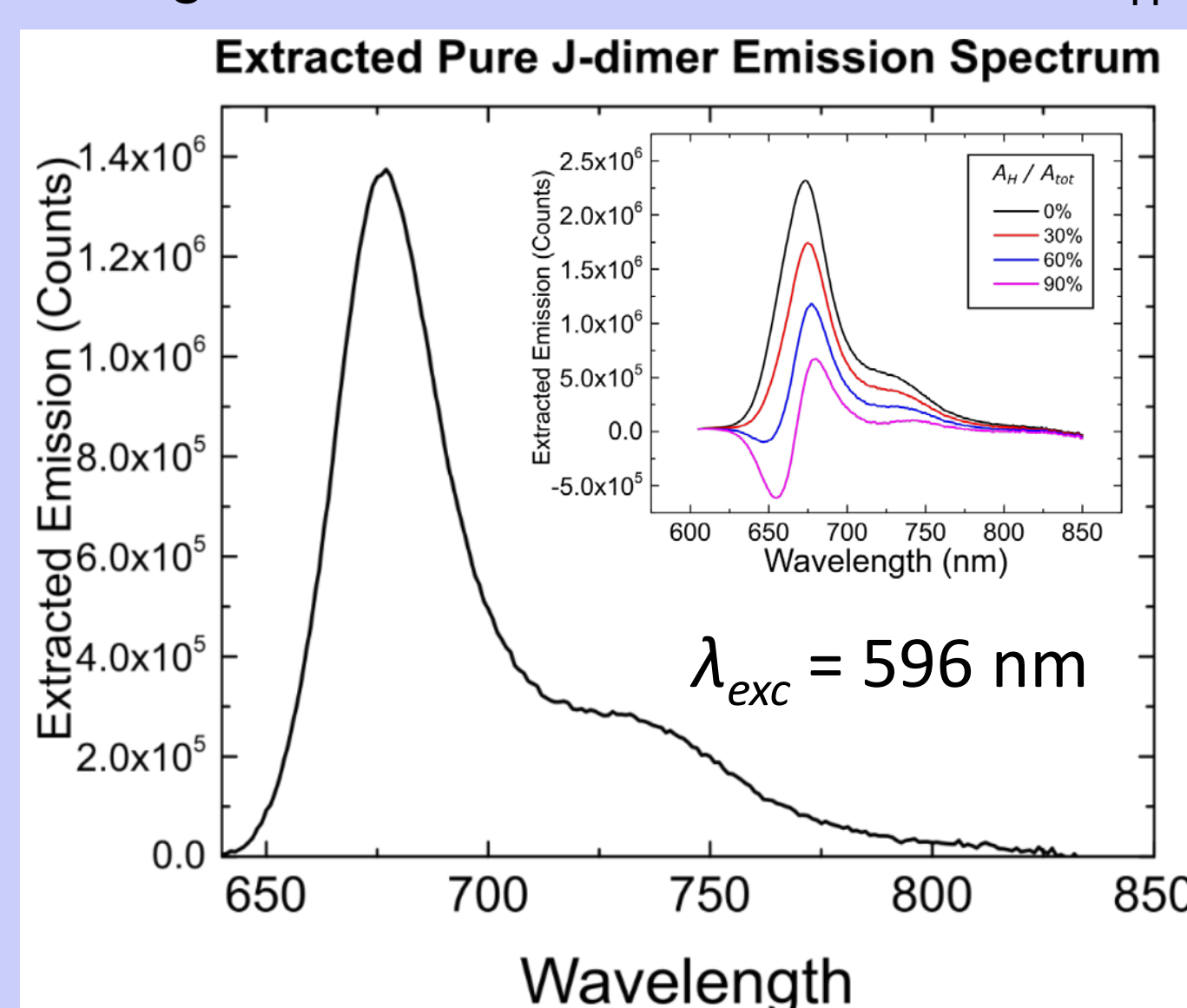
- For the three-component J-dimer solution, the equation for fluorescence quantum yield,  $\Phi_{F, Tot}(\lambda)$ , has three terms:

$$\Phi_{F, Tot}(\lambda) = \left( \frac{A_m(\lambda)}{A_{Tot}(\lambda)} \right) \Phi_{F, m} + \left( \frac{A_J(\lambda)}{A_{Tot}(\lambda)} \right) \Phi_{F, J} + \left( \frac{A_H(\lambda)}{A_{Tot}(\lambda)} \right) \Phi_{F, H}$$

**Equation 1.** Expression for the fluorescence quantum yield of the three-component J dimer solution.  $A_n(\lambda)$  is the absorbance at wavelength  $\lambda$  of solution component  $n$ ,  $A_{Tot}(\lambda)$  is the total absorbance of the solution at excitation wavelength,  $\lambda$ .  $\Phi_{F, n}$  is the fluorescence quantum yield of solution component  $n$ , while  $\Phi_{F, Tot}(\lambda)$  is the fluorescence quantum yield of the solution at excitation wavelength,  $\lambda$ .

- By making the assumption that the H-aggregate component is nonfluorescent ( $\Phi_{F, H} = 0$ ), the expression above can be solved with a single fitting parameter,  $A_H$ .
- Because  $\Phi_{F, m}$  and  $\Phi_{F, Tot}$  can be measured directly, a narrow bounded approximation of  $\Phi_{F, J}$  can be made based on the monomer radiative rate (see part 5).
- $A_H$  was allowed to float in order to solve for  $A_m$ , which was used to scale and subtract a monomer emission spectrum from the J-dimer solution emission spectrum.
- A realistic J-dimer emission spectrum (all positive, similar peak width to J-dimer absorption spectrum) emerges from the subtraction when  $A_H$  is 49% of  $A_{Tot}(\lambda)$ .

**Figure 4.** The emission spectrum which resulted from the extraction procedure. The half width at half max (HWHM) of the J-dimer origin band was used along with the constraint that the whole spectrum must be positive to fix the value of  $A_H$ . **Inset.** Multiple extractions for different values of  $A_H$  return less physically realistic emission spectrum extractions, presenting either very broad peaks for  $A_H = 0$  or negative features for  $A_H > 60\%$



## 5. ESTIMATION OF $k_{NR}$ AND $k_r$ FOR J-DIMER

- Because the physical size of the J-dimer is restricted to two monomer units, the maximum radiative rate of the J-Dimer,  $k_{r, J}$ , is twice that of the Cy5 monomer [5].
- Based on the FQY and kinetics of the Cy5 monomer, the radiative rate,  $k_r$ , of the monomer can be determined, allowing for a narrow approximation of  $k_r$  for the J-dimer.
- Figure 5 shows the expected excited state dynamics of the J-Dimer assuming  $k_{nr}$  does not change upon aggregation.

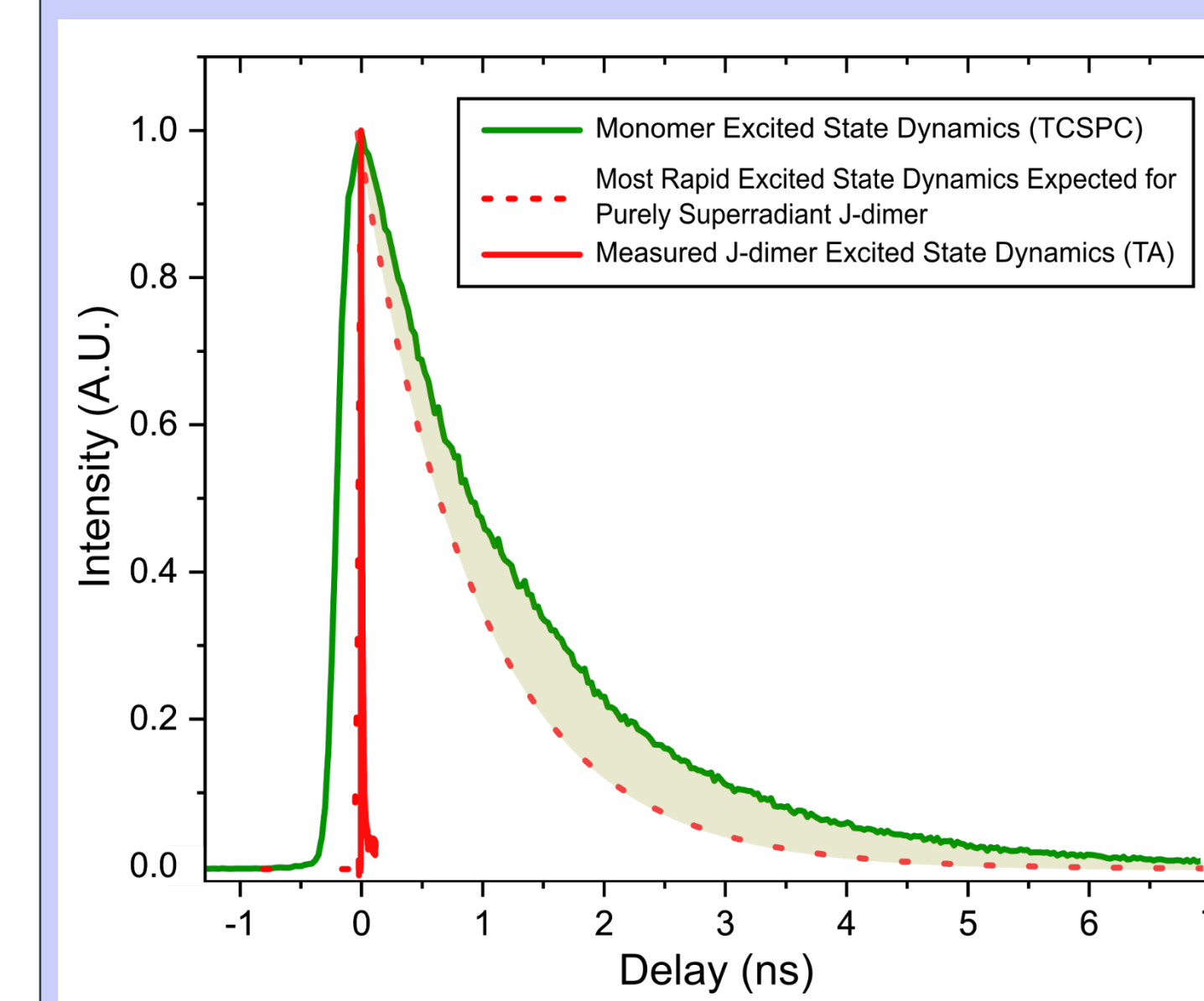


**Figure 5.** Measured (solid red) and expected (dashed red) excited state kinetics for the J-dimer. The Cy5 monomer kinetics (solid green) as measured by time resolved single photon counting (TCSPC) forms the upper bound of the expected J-dimer kinetics. The lower bound (red dashed line) with a time constant of 1 ns represents the fastest expected kinetics based on a doubling of the monomer radiative rate under the assumption of full superradiance (e.g.,  $n_{coh} = 2$ ). The two traces form a bounded area representing possible J-dimer lifetimes under the assumption that  $k_{nr, J} = k_{nr, m}$ . The actual J-dimer relaxation kinetics as measured by transient absorption spectroscopy are much more rapid than is expected for the case of superradiance only.

- More rapid decay beyond the shaded region in Figure 5 can only be accounted for by an increase in the nonradiative relaxation rate (relative to the Cy5 monomer) upon aggregation.
- The ground state recovery rate of the J-dimer was nearly 100-fold faster than expected, indicating that its relaxation is almost entirely nonradiative, a conclusion that is further supported by the low fluorescence measured from J-dimer solutions relative to the monomer.
- Table 1 provides a summary of the photophysical properties of the monomer, J-Dimer, and H-Tetramer, including a quantitative evaluation of the extent to which nonradiative decay contributes to the overall decay.

**Table 1.** Fluorescence Quantum Yields, Overall Lifetimes, and Overall, Radiative, and Nonradiative Decay Rates for Cy5 Monomer, J-dimers, and H-tetramers

Sample	$\Phi_F$	$\tau_{obs}$ (ns)	$k_{obs}$ (s <sup>-1</sup> )	$k_r$ (s <sup>-1</sup> )	$k_{nr}$ (s <sup>-1</sup> )	$k_{nr}/k_{obs}$ (%)
MonomerA	0.29	1.3	$7.69 \times 10^8$	$2.23 \times 10^8$	$5.46 \times 10^8$	71.00
J-dimer (N = 1.5)	N/A	0.011	$9.09 \times 10^{10}$	$3.34 \times 10^8$	$9.06 \times 10^{10}$	99.63
H-tetramer	N/A	0.035	$2.86 \times 10^{10}$	$1.12 \times 10^7$	$2.86 \times 10^{10}$	99.96

## 6. REFERENCES & ACKNOWLEDGMENTS

### References

- [1] E. E. Jelley. Nature 1936,138,1009; [2] E. E. Jelley. Nature 1937, 139, 631; [3] G. Scheibe. Angew. Chem. 1937, 50, 212; [4] F. Würthner *et al.* Angew. Chem. Int. Ed. 2011, 50, 3376; [5] F. Spano *et al.* J. Chem. Phys. 1989, 91 (2), 683; [6] A. T. Haedler *et al.* Nature 2015, 523, 196; [7] B. L. Cannon *et al.* J. Phys. Chem. A2018, 122, 2086; [8] B. L. Cannon *et al.* J. Phys. Chem. A2017, 121, 6905; [9] P. D. Cunningham *et al.* J. Phys. Chem. B 2018, 122, 5020; [10] J. L. Banal *et al.* J. Phys. Chem. Lett. 2017, 8, 5827; [11] E. Boulais *et al.* Nat. Mater. 2018, 17, 159; [12] J. S. Huff *et al.* J. Phys. Chem. Lett. 2019, 10, 2386.

### Acknowledgments

Work at Boise State University was supported by the NSF INSPiRE No. 1648655 and NSF MRI Award 0923541. Portions of this work were also supported by the Department of Energy (DOE), LDRD No. 154754. Z.S.D.T. and G.D.S. acknowledge support from the Division of Chemical Sciences, Geosciences, and Biosciences, Office of Basic Energy Sciences of the U.S. DOE, through Grant No. DE-SC0019370. We thank the students and staff within the Nanoscale Materials & Device Research Group ([nano.boisestate.edu](http://nano.boisestate.edu)).